JNeurosci Accepted Manuscript

JNeurosci
THE JOURNAL OF NEUROSCIENCE

Research Articles: Development/Plasticity/Repair

Emotional stress induces structural plasticity in Bergmann glial cells via an AC5-CPEB3-GluA1 pathway

https://doi.org/10.1523/JNEUROSCI.0013-19.2020

Cite as: J. Neurosci 2020; 10.1523/JNEUROSCI.0013-19.2020

Received: 21 December 2018
Revised: 13 February 2020
Accepted: 27 February 2020

This Early Release article has been peer-reviewed and accepted, but has not been through the composition and copyediting processes. The final version may differ slightly in style or formatting and will contain links to any extended data.

Alerts: Sign up at www.jneurosci.org/alerts to receive customized email alerts when the fully formatted version of this article is published.

Copyright © 2020 Bender et al.

JNeurosci Accepted Manuscript

1 **Emotional stress induces structural plasticity in Bergmann glial cells via an AC5-CPEB3-GluA1 pathway**

2 Authors: Crhistian Luis Bender[1,4,6], Xingxing Sun[1,5,6,7], Muhammad Farooq[1,7], Qian Yang[1], Caroline
3 Davison[1], Matthieu Maroteaux[1], Yi-shuian Huang[2], Yoshihiro Ishikawa[3], Siqiong June Liu[1,7]

4 [1]Department of Cell Biology and Anatomy, LSUHSC, New Orleans, LA, USA

5 [2]Institute of Biomedical Sciences, Academia Sinica, Taipei, Taiwan

6 [3]Cardiovascular Research Institute, Yokohama City University Graduate School of Medicine, Yokohama,
7 Japan

8 [4]Present address: Insituto de Farmacología Experimenta de Córdoba-CONICET. Departamento de
9 Farmacología, Facultad de Ciencias Químicas, Universidad nacional de Córdoba, Argentina.

10 [5]Present address: Department of Anesthesiology, Tongji Hospital, Tongji Medical College, Huazhong
11 University of Science & Technology, Wuhan, China

12 [6] These authors made equal contributions.

13 [7] Southeast Louisiana VA Healthcare System, New Orleans, LA, 70119, USA

14

15 **Correspondence should be addressed to:**

16 Dr. Siqiong June Liu

17 Department of Cell Biology and Anatomy

18 Louisiana State University Health Sciences Center

19 New Orleans, LA 70112

20 e-mail: sliu@lsuhsc.edu

21 Phone #: (504)-568-2258

22 Fax #: (504) 568-2169

23

24 Acknowledgements: This work was supported by National Institutes of Health Grants NS58867,
25 MH095948 and R01NS106915 (S.Q.J.L.), an NIH COBRE grant P30 GM106392 and T35DK093428, and VA
26 grant BX003893. We would like to thank Ms Jessica Patel, Drs Charles Nichols, Matthew Whim,
27 Christophe J. Dubois, Iaroslav Savtchouk and Kathryn L. Carzoli for their technical advice and helpful
28 discussions.

29

30

JNeurosci Accepted Manuscript

33 **ABSTRACT**

34 Stress alters brain function by modifying the structure and function of neurons and astrocytes. The fine
35 processes of astrocytes are critical for the clearance of neurotransmitters during synaptic transmission.
36 Thus, experience-dependent remodeling of glial processes is anticipated to alter the output of neural
37 circuits. However, the molecular mechanism(s) that underlie glial structural plasticity are not known.
38 Here we show that a single exposure of male and female mice to an acute stress produced a long-lasting
39 retraction of the lateral processes of cerebellar Bergmann glial cells. These cells express the GluA1
40 subunit of AMPA-type glutamate receptors and GluA1 knockdown is known to shorten the length of glial
41 processes. We found that stress reduced the level of GluA1 protein and AMPA receptor-mediated
42 currents in Bergmann glial cells and these effects were absent in mice devoid of CPEB3, a protein that
43 binds to GluA1 mRNA and regulates GluA1 protein synthesis. Administration of a β-adrenergic receptor
44 blocker attenuated the reduction in GluA1 and deletion of adenylate cyclase 5 prevented GluA1
45 suppression. Therefore, stress suppresses GluA1 protein synthesis *via* an adrenergic/adenylyl
46 cyclase/CPEB3 pathway, and reduces the length of astrocyte lateral processes. Our results identify a
47 novel mechanism for GluA1 subunit plasticity in non-neuronal cells, and suggest a previously
48 unappreciated role for AMPA receptors in stress-induced astrocytic remodeling.

49

50 Significance statement

51 Astrocytes play important roles in synaptic transmission by extending fine processes around synapses. In
52 this study, we showed that a single exposure to an acute stress triggered a retraction of lateral/fine
53 processes in mouse cerebellar astrocytes. These astrocytes express GluA1, a glutamate receptor subunit
54 known to lengthen astrocyte processes. We showed that astrocytic structural changes are associated
55 with a reduction of GluA1 protein levels. This requires activation of β-adrenergic receptors and is
56 triggered by noradrenaline released during stress. We identified adenylyl cyclase 5 as a downstream
57 effector, an enzyme that elevates cAMP levels, and found that lowering GluA1 levels depends on CPEB3
58 proteins that bind to GluA1 mRNA. Therefore, stress regulates GluA1 protein synthesis via an
59 adrenergic/adenylyl cyclase/CPEB3 pathway in astrocytes and remodels their fine processes.

60

61

62

63

JNeurosci Accepted Manuscript

64 **INTRODUCTION**

65 Stress modifies the structure and function of neurons and glial cells in the brain, producing lasting
66 changes in behavior and physiology. This is significant because the experience of traumatic events can
67 lead to neuropsychiatric disorders (McEwen and Gianaros, 2010; Franklin et al., 2012) including anxiety,
68 depression and drug addiction (Shin and Liberzon, 2010; Edwards et al., 2013; Papp et al., 2014). While it
69 is established that stress can alter the spine density, the dendritic length and complexity in neurons
70 (Christoffel et al., 2011; Davidson and McEwen, 2012), astrocytes, which are a critical component of
71 synaptic transmission, can also undergo structural changes. The fine processes of astrocytes contact pre-
72 and postsynaptic sites, where glutamate transporters in astrocytes rapidly remove glutamate released
73 from presynaptic terminals (Araque et al., 1999). It is therefore not surprising that they are essential for
74 stress-related behavior. For example, astrocyte ablation in the prefrontal cortex gives rise to depression-
75 like behaviors and chronic stress reduces the number of astrocytes and their main branches (Banasr and
76 Duman 2008; Tynan et al., 2013). Given the importance of astrocyte processes in neurotransmitter
77 clearance, their retraction is expected to prolong the presence of glutamate at the synaptic site and
78 enhance transmission. However, how stress remodels the structure of astrocytes is still poorly
79 understood (Bender et al., 2016).

80 Exposure of rodents to natural predator odors causes innate fear (Takahashi et al., 2005; Staples, 2010)
81 and the cerebellum is involved in the processing of the fear response to predators as lesions of the
82 cerebellar vermis reduce a freezing response in rats exposed to a cat (Supple et al., 1987). There are
83 extensive connections between the cerebellum and brain regions that are important for defense
84 responses, including the limbic, prefrontal cortex and sympathetic nervous systems (Bostan et al., 2013).
85 Exposure to predator odor evokes norepinephrine release from the locus coeruleus and we have
86 previously shown that this increases GluA2 transcription in cerebellar stellate cells and enhances
87 feedforward inhibition (Liu et al., 2010; Savtchouk and Liu, 2012). The cerebellum is also critical for the
88 consolidation of associative fear conditioning (Fischer et al., 2000; Sacchetti et al., 2002; Timmann et al.,
89 2010). Therefore, a stress-induced change in synaptic transmission in the cerebellum may alter the
90 processing of emotion and fear memory.

91 Bergmann glial cells in the cerebellum have lateral, fine processes surrounding both excitatory and
92 inhibitory synapses in the molecular layer and regulate synaptic transmission (Ango et al., 2008; De
93 Zeeuw and Hoogland, 2015). Retraction of these processes can lead to motor deficits (Saab et al., 2012).
94 Because stress is a common trigger for cerebellar ataxia (Jen, 2000), we examined whether stress
95 altered the size of the glial processes. These astrocytes express a high level of GluA1 subunits that form
96 Ca^{2+} permeable AMPA receptors. Selective expression of GluA2 and knockdown of the GluA1 subunit in
97 Bergmann glial cells reduces the length of their processes and impairs motor coordination (Iino et al.,
98 2001; Saab et al., 2012). Thus the ability of emotional stress to regulate GluA1 expression in astrocytes
99 suggests a mechanism for controlling the length of Bergmann glial processes.

100 Our results show that a single exposure to predator odor produces a lasting reduction in the length of
101 Bergmann glial lateral processes and a decrease in GluA1 expression and AMPA receptor-mediated
102 currents in glial cells. We found that deletion of CPEB3, a protein that binds to GluA1 mRNA, prevented

JNeurosci Accepted Manuscript

103 the suppression of GluA1 protein levels and a decrease in the current via AMPA receptors, suggesting
104 stress reduces GluA1 protein synthesis in Bergmann glial cells. Blocking β-adrenergic receptors during
105 emotional stress attenuates the reduction in GluA1 levels, and deletion of adenylyl cyclase 5 abolishes
106 the change in GluA1 expression. Therefore, acute stress suppresses GluA1 expression via activation of a
107 β adrenergic receptor-AC5 pathway that requires CPEB3. Our results reveal a new form of GluA1 subunit
108 plasticity in astrocytes and suggests a novel role for AMPA receptors in stress-induced astrocytic
109 remodeling.

110 MATERIALS AND METHODS

111 ANIMALS

112 We used 5-8 week old C57BL/6J NPY::GFP (Jackson Laboratory, stock #: 006417) mice for the
113 morphological analysis of Bergmann glial cells because GFP is expressed in scattered BG cells in this
114 mouse line. FVB/NJ GFAP::GFP (Jackson Laboratory; stock #: 003257) mice were used for the analysis of
115 GluA1 immunoreactivity (ir) in the molecular and Purkinje cell layers occupied by the processes and
116 somata, respectively of Bergmann glial cells. Adenylyl cyclase 5 (AC5) knock out (KO), C57BL/6J CPEB3
117 (Cytoplasmic Polyadenylation Element Binding protein 3) KO mice and their wild-type controls were
118 used for immunohistochemical and electrophysiological experiments. In all experiments, both male and
119 female animals were used. We did not observe any difference in the stress-induced change in GluA1-ir in
120 5-6 week old (81±2%) and 7-8 week old (84±1%) mice ($t_{16} = -0.6$; $p = 0.56$), and therefore data were
121 pooled from these animals. All procedures were approved by the Animal Care and Use Committee of
122 Louisiana State University Health Sciences Center.

123 STRESS PARADIGM

124 Mice were exposed to fox urine as described previously (Liu et al., 2010). Briefly, a mouse was placed in
125 a cage (13 × 9 × 6 inches) for 2 minutes. A paper towel containing fox urine (2.5 ml) was then inserted
126 below the raised floor which contained small holes allowing the odor to permeate into the chamber. The
127 animal was exposed to odor for 5 minutes, then returned to their home cage and sacrificed 3 or 24 hs
128 later. Care was taken to minimize handling stress. Control (“naive”) animals were left undisturbed in
129 their home cage.

130 PHARMACOLOGICAL EXPERIMENTS

131 Mice were exposed to fox urine 30 minutes after the intraperitoneal injection of saline or propranolol
132 (20 mg/kg; dissolved in saline; injection volumes: 0.1 ml/15 g body weight). Home cage animals that did
133 not receive an injection, and stressed animals were littermates of same sex. Naïve mice receiving a
134 saline or propranolol injection or no injection served as additional controls. At 24 hours after exposure
135 to fox urine, animals were euthanized, then perfused with paraformaldehyde and the brains processed
136 for GluA1 staining as described below.

137 HISTOLOGY AND IMMUNOHISTOCHEMISTRY

JNeurosci Accepted Manuscript

138 NPY::GFP mice, which express GFP in Bergmann glial cells, were used to determine the length of glial
139 processes. Animals were perfused intracardially with 10 ml of heparinized PBS followed by 20 ml of 4%
140 paraformaldehyde. The brains were post-fixed overnight in paraformaldehyde, then kept in 25% sucrose
141 in PBS. Cerebellar slices of 30 µm were cut with a cryostat at -20 °C, collected in wells containing PBS
142 and mounted on slides.

143 For immunohistochemistry, animals were intracardially perfused with 10 ml of heparinized PBS followed
144 by 50 ml of 4% paraformaldehyde with a peristaltic pump (2 ml/min). The brains were post-fixed
145 overnight in paraformaldehyde solution and then kept in PBS at 4°C. Cerebellar slices of 50 µm were
146 obtained using a vibratome. Free-floating sections were pre-incubated in blocking / permeabilization
147 solution (PBS containing 5% BSA and 0.1 % Triton X-100) for 2 hours at room temperature. The slices
148 were then incubated with primary antibodies overnight. After 5 washes in PBS (10 min each) the
149 sections were incubated with secondary antibodies for 2 hours at room temperature, then were washed
150 5 times and mounted on slides. Slides were dried and sections were mounted in Vectashield. Antibodies
151 were diluted in PBS that contained 1% BSA and 2% donkey serum. To detect CPEB3-immunoreactivity,
152 antigen retrieval was conducted in 10 mM sodium citrate solution (pH 6) at 95°C for 30 minutes.
153 Sections were washed twice in PBS, then followed by the standard immunostaining procedure.

154 Primary antibodies: rabbit anti GluA1 (1:1000, Chemicon; Cat#: AB1504 1), mouse anti CPEB3 (1:200
155 Chao et al.,2013), rabbit anti GFAP (1:500, DAKO), chicken anti-GFP (1:500, Santa Cruz), rabbit anti-AC
156 V/VI (1:500, Santa Cruz, Cat#: sc-590). Secondary antibodies: Cy3 donkey anti-mouse (1:400, Jackson),
157 Alexa 488 goat-anti chicken (1:400, Invitrogen), Alexa 488 donkey anti rabbit (1:400, Invitrogen), Cy3
158 donkey anti-rabbit (1:400, Jackson), Alexa 488 goat anti mouse (1:400, Invitrogen).

159 IMAGE AQUISITION AND ANALYSIS

160 Morphological analysis of Bergmann glial cells: images of GFP fluorescence were acquired with a TCS SP2
161 SE Leica confocal microscope at 63x plus 2x camera optical zoom, a step size of 0.5 µm and 1024x1024
162 pixel resolution. The final thickness of each stack varied between 18-25 µm. In NPY::GFP mice, a subset
163 of Bergmann glial cells express GFP and their scattered distribution allows for individual cells to be
164 photographed for analysis of lateral processes. From each animal at least 3 cells in lobule 5 of the
165 cerebellar vermis were photographed. The length of 40 lateral processes arising from the main glial
166 branches were measured from each image and the average length of 120 processes from 3 images was
167 calculated for each animal. 7-8 mice were used for each experimental condition.

168 For lateral process length analysis, a 3-D reconstruction was made using Leica software (Leica
169 microsystems Heidelberg GmbH 1997-2004). Rotation of the image facilitated the differentiation of the
170 main processes (usually 3-5 main branches) from their respective lateral processes. The length of any
171 single, clearly identifiable, lateral process that emanated from the principal process was manually traced
172 and quantified using ImageJ with the aid of a pair of 3-D glasses. Lateral processes that contained
173 smaller processes giving a final brush-like appearance were not considered in this analysis because of
174 their complexity and heterogeneity. The brush-like pattern was more prominent in the superficial third
175 of the molecular layer (proximal to the surface and distant from the somatic layer) hence most of the

JNeurosci Accepted Manuscript

176 measurements were conducted in the inner 2/3 of the molecular layer. The samples were coded and the
177 analysis was conducted blind to the experimental conditions.

178 To confirm that our manual measurement of glial process length was random and non-biased, we
179 assessed the morphological changes using skeleton analysis. The same image stacks used for 3-D
180 reconstruction were used to create single max projected images that were subject to visual thresholding
181 and then skeletonization with ImageJ software. The skeleton analysis plug-in was applied to obtain the
182 length of all branches found in the skeleton (Arganda-Carreras et al., 2010). No pruning algorithm was
183 applied but we discarded all processes that were shorter than 1 µm and longer than 10 µm which was
184 the size range of the processes obtained with the free hand manual measurements. The drawback of
185 this approach is that projection of a 3D image onto a 2D plane would reduce the length of processes that
186 are outside of the projection plane. Indeed, the average length of process in both control and after
187 stress were smaller overall than in the manual measurement protocol and the number of processes was
188 higher. However the relative change in the length of processes after stress was the same as found using
189 the manual measurement approach. The Pearson correlation coefficient between the average length of
190 glial processes from each animal using manual measurements and skeleton analysis was 0.72
191 ($p<0.0001$). A good match between both methods validates our manual measurements as a non-biased
192 approach. Because skeleton analysis underestimates the length of glial processes, the manual measure
193 was used in our study.

194 Analysis of GluA1 and CPEB3 immunoreactivity: Images were acquired with an epifluorescence
195 microscope (Nikon Eclipse TE2000-U) at 10x magnification. Lobules 5 and 9 from the cerebellar cortex
196 were analyzed from at least 5 sections per animal. The sections selected for analysis were matched with
197 sagittal diagrams located between 0.12-0.36 lateral to the midline in the Paxinos and Franklin mouse
198 atlas (2001) (see Figure 1D). The mean intensity of staining in the molecular, granule and Purkinje layers
199 was quantified using ImageJ. Because GluA1 is expressed in Bergmann glial cells but not in granule cells,
200 GluA1-immunoreactivity in the granule cell layer was considered as background and was subtracted
201 from the values obtained in the molecular layer, where the processes of BG are found, and from the
202 Purkinje cell layer where the BG soma are located. The divisions between the Purkinje cell layer and
203 molecular or granule cell layer were guided using the GFAP::GFP signal present in the BG somata. In
204 each figure, the symbols indicate the mean value from each animal. Identical symbols are used for the
205 same sex littermate control and stressed animals from each independent experiment. GluA1-ir was
206 normalized to the average value of the naïve control from the same batch of animals to account for the
207 variability in staining intensity between different batches of animals. To determine whether
208 immunostaining of GluA1 and CPEB3 was co-localized with GFAP-ir or GFP in GFAP::GFP mice, confocal
209 images were acquired using a TCS SP2 SE Leica confocal microscope (63x objective). Maximum projected
210 images were produced from a stack of images at a step size of 0.5 um (resolution 1024x1024) and used
211 for analysis.

212 Electrophysiological recordings: Cerebellar slices were prepared from 25-35 day old naïve mice or mice
213 that were exposed to fox urine 24 hrs previously, as described (Savtchouk and Liu, 2011). Briefly,
214 horizontal slices (300 µm) were cut from the cerebellar vermis using a vibratome (Leica VT1200) in ice-
215 cold solution containing (mM): $CaCl_2$ (0.5), NaCl (81.2), KCl (2.4), $NaHCO_3$ (23.4), NaH_2PO_4 (1.4), 6.7 $MgCl_2$

JNeurosci Accepted Manuscript

216 (6.7), glucose (23.3), sucrose (69.9) and gassed with carbogen (95% O_2/5% CO_2). Slices were then
217 transferred to aCSF solution containing (mM): NaCl (125), KCl (2.5), $NaHCO_3$(26), NaH_2PO_4(1.25), $MgCl_2$
218 (1), $CaCl_2$ (2), glucose (25) and saturated with 95% O_2, 5% CO_2 at room temperature for at least 30 min
219 before recording. Recording pipettes (4-7 MΩ) were pulled from borosilicate capillary glass (GC150F-7.5,
220 Harvard Apparatus, Holliston, MA) with a Narishige PP-830 puller and were filled with a potassium-
221 based internal solution (mM): $MgCl_2$ (2), HEPES (10), CH_3KO_3S (140), EGTA (0.5), Na-ATP(2). The
222 stimulation pipettes were fabricated from thin-wall borosilicate capillary glass (GC150TF-10, Harvard
223 Apparatus, Holliston, MA) and filled with aCSF.

224 Bergman glial cells were identified by the size and location of somata in the Purkinje cell layer, and a
225 hyperpolarized resting membrane potential (~-80mV) immediately after obtaining the whole cell patch
226 clamp configuration. Whole cell voltage-clamp recordings were obtained from cerebellar Bergmann glial
227 cells in lobule 5/6, at -80mV, using a Multiclamp 700A (Axon Instruments), and currents were filtered at
228 10 kHz and digitized at 20 kHz. Parallel fibers were stimulated using a thin-wall pipette positioned within
229 the molecular layer (20-30V, 200 µs pulse), and membrane currents in Bergman cells were recorded in
230 response to stimuli. Series resistance compensation (≥60%) was applied to minimize voltage errors
231 during recordings. A non-NMDAR inhibitor (10 µM NBQX) was applied through the perfusion system
232 after a 5 min stable baseline recording. Data acquisition and analysis were performed using pClamp 9.0
233 (Axon Instruments). Series resistance, input resistance and cell capacitance were monitored throughout
234 the recording and these were discarded if the parameters changed by more than 20%.

235 STATISTICS

236 The Kolmogorov–Smirnov test was used for analyzing the cumulative distribution of the length of
237 Bergmann glial cell processes. We used a two-tailed unpaired Student's t test to compare normalized
238 GluA1 immunoreactivity (GluA1-ir) in littermates (naive vs stress) that were processed in parallel and to
239 compare the stress-induced change in GluA1-ir between two genotypes or pharmacological treatment
240 groups. We analyzed the effect of stress on GluA1 expression by normalizing GluA1-ir in naïve and
241 stressed mice either to the batch average of naïve GluA1-ir, or to the average GluA1-ir within each pair
242 (stressed and naïve littermates; = ($GluA1\text{-}ir_{naive}$ + $GluA1\text{-}ir_{stressed}$)/2). Statistical analysis of these two sets
243 of data using unpaired Student's t test were comparable and we therefore present only the GluA1-ir
244 result normalized to the batch average of naïve GluA1-ir in Figures 2, 3, 5 and 8. Only normalized GluA1-
245 ir values in stressed mice are reported in the text of the Results section. A repeated measures ANOVA
246 was used to compare the intensity of GluA1-ir among different lobules. An unpaired t-test was used for
247 comparison of AMPA receptor–mediated currents in naive mice and after stress. Data are presented as
248 mean ± SEM and the n value is the number of animals unless otherwise indicated. Data were considered
249 to be significantly different if $P < 0.05$.

250

251

JNeurosci Accepted Manuscript

252 **RESULTS**

253 **Acute stress reduces the length of Bergmann glial cell lateral processes**

254 The cerebellum is critical for both motor coordination and non-motor functions, with different
255 cerebellar lobules being involved in distinct behaviors. The formation of fear memory requires the
256 activity of cerebellar vermal lobule 5, and motor learning involves lobules 9/10 (Sacchetti et al., 2002a,
257 2004; Ruediger et al., 2011). Because stress can enhance subsequent fear learning and memory (Perusini
258 et al., 2016), we examined whether exposure to predator odor altered the length of Bergmann glial cell
259 processes in lobule 5, a region that is critically involved in fear memory consolidation.

260 Bergmann glial (BG) cells have 2-4 primary processes, from which fine processes then extend laterally
261 and which form close contacts with both excitatory and inhibitory synapses in the molecular layer of the
262 cerebellum. To measure the length of the lateral branches emanating from the main processes we took
263 advantage of a transgenic NPY::GFP mouse line in which GFP is selectively expressed in scattered BG
264 cells within the cerebellar cortex (Figure 1A). This enabled us to perform single cell 3D reconstructions
265 and to recognize and quantify the length of individual lateral processes.

266 To determine whether acute stress altered the size of the glial processes, NPY::GFP mice were exposed
267 to fox urine for 5 minutes and cerebella were fixed 3 or 24 hours later. In naive mice the average length
268 of BG lateral processes in lobule 5 was 2.80 ± 0.22 µm (n = 8). In contrast, the length of processes in
269 mice that were exposed to predator odor stress was reduced to 2.4 ± 0.14 µm (n = 7), when evaluated 3
270 hours after exposure (Figure 1B-C). The distribution of the size of individual process showed that
271 stressed animals had shorter lateral processes than naive controls (Figure 1C, naive: 24 cells and 891
272 processes; stress 3 hrs: 22 cells and 914 processes; Kolmogorov- Smirnov (K-S) test: naive vs stress 3hrs,
273 $p<0.0001$). At 24 hours after stress the length of the lateral processes was further reduced to 2.26 ± 0.08
274 µm (n = 7) (Figure 1B-C, stress 24hrs: 22 cells and 836 processes; vs naive, K-S test: $p<0.000001$),
275 compared to 3hrs after stress (K-S test: $p<0.0001$). Thus, a single emotional stress was able to induce a
276 sustained retraction of glial processes that lasted for at least 24 hrs, a form of structural plasticity in
277 cerebellar astrocytes.

278 **GluA1 expression in Bergmann glial cells decreases after acute emotional stress**

279 Bergmann glial cells express high levels of GluA1 subunits which form Ca^{2+} permeable AMPA receptors.
280 Knockdown of GluA1 and over-expression of GluA2 in BG cells decreases the expression of Ca^{2+}
281 permeable AMPA receptors and reduces the length of the lateral processes (Iino et al., 2001; Saab et al.,
282 2012). We hypothesized that the shortening of lateral processes after stress could result from a down-
283 regulation of GluA1 expression. Using immunohistochemistry we detected GluA1-ir in the cerebellar
284 cortex, where GluA1 is almost exclusively expressed in BG cells (Petralia and Wenthold, 1992). We found
285 that GluA1 immunostaining in GFAP::GFP mice was localized to GFP positive processes and BG somata,
286 with little staining of stellate and a low level of GluA1-ir in the soma of Purkinje cells, and no staining
287 above background in the granule cell layer (Figure 2A) as previously reported (Petralia and Wenthold,
288 1992; Baude et al., 1994).

JNeurosci Accepted Manuscript

289 We next quantified the level of GluA1-ir in the molecular layer since the processes of BG cells extend
290 from the Purkinje cell layer, through the molecular layer, and terminate as end-feet on the surface of
291 the cerebellar cortex (Figures 1D and 2B). Compared to naive controls, the average GluA1
292 immunoreactivity in the molecular layer of lobule 5 decreased by 21% in mice 24 hours after fox urine
293 exposure (stress: 0.79±0.13; unpaired t-test: t(10) = -3.12, p<0.011), indicating a reduction in GluA1
294 protein after stress. This change occurred selectively in the molecular layer in lobule 5 because no
295 difference was observed in the BG somatic layer (stress: 1.01±0.11; unpaired t-test: t(10) = -0.17,
296 p=0.871), or the molecular layer in lobule 9 (stress: 0.90±0.2; unpaired t-test t(10) = 1.05, p=0.319)
297 (Figure 2C). Furthermore, stress did not alter GFP expression in the molecular layer in lobule 5 (stress:
298 0.92±0.1; unpaired t-test: t(6) = 1.40, p=0.210).

299 Exposure to fox urine reduced the length of Bergmann glial cells lateral processes, and this was detected
300 as early as 3hrs after stress (Fig 1). We therefore determined the level of GluA1-ir 3hr following stress in
301 C57BL/6J mice. We found that GluA1 immunoreactivity in the molecular layer of lobule 5 was reduced
302 by 16 % (stress: 0.84±0.11; unpaired t-test: t(6) = 2.68, p=0.036), but not in lobule 9 (Fig 3A-C). The
303 decrease in GluA1 expression (=100%*(GluA1-ir_{stress})/GluA1-ir_{naive}) persisted as the level of GluA1-ir level
304 remained suppressed 24 hrs after fox urine exposure (% change at 3 vs 24 hrs: unpaired t-test: t(8)=-
305 0.67, p = 0.519) (Fig 3D). Therefore, predator odor stress induced a rapid and sustained decease in
306 GluA1 expression.
307
308 As a second independent approach, we tested whether stress altered AMPA receptor-mediated currents
309 in Bergmann glial cells from C57BL/6J mice. Stimulation of parallel fibers evokes release of glutamate,
310 and activates AMPA receptors and glutamate transporter activity in these cells, producing an inward
311 current (Clark and Barbour, 1997). We made whole cell patch clamp recordings from Bergmann glial
312 cells in vermal lobule 5 and detected an inward membrane current immediately following parallel fiber
313 activation (Fig 4A). To isolate the component of this current that was mediated via AMPA receptors, we
314 applied NBQX, a non-NMDA receptor blocker, and found that the current amplitude was rapidly reduced
315 reaching a plateau after 5-10 min. From these experiments we conclude that AMPA receptors mediate
316 about 35% of the parallel fiber-evoked current in Bergmann cells from naïve mice, consistent with a
317 previous report (Clark and Barbour, 1997). To determine the effects of stress on this current, we
318 exposed mice to fox urine, and prepared cerebellar slices the next day and quantified the parallel fiber-
319 stimulation evoked currents. In this condition, application of NBQX blocked 19.9% of the inward current
320 in Bergmann cells, a markedly smaller inhibition compared to naïve controls (unpaired t-test
321 t(10)=4.030, P=0.0024. Fig 4B and 4C). This reduced inhibition by NBQX indicates a decrease in AMPA
322 receptor-mediated current in these astrocytes after acute stress. Therefore, predator odor stress
323 lowered the expression level of GluA1 protein and reduced the amplitude of the AMPA receptor-
324 mediated current in Bergmann glial cells.

325 **Deletion of CPEB3 prevents the stress-induced reduction in GluA1 expression in Bergmann glial cells**

326 The synthesis of GluA1 is regulated by an RNA binding protein, CPEB3 (cytoplasmic polyadenylation
327 binding protein 3) that suppresses the translation of GluA1 (Chao et al., 2013; Drisaldi et al., 2015). Thus
328 stress may reduce GluA1 protein levels *via* a CPEB3-dependent pathway in Bergmann glial cells. We

JNeurosci Accepted Manuscript

329 observed CPEB3-ir in Bergmann glial-like processes and in interneurons in the molecular layer, and this
330 staining was abolished in CPEB3 knockout mice (Figure 5A). Double immunolabeling with GFAP and
331 CPEB3 antibodies showed a co-localization of CPEB3- with GFAP-ir (Figure 5A). Thus Bergmann glial cells
332 express the CPEB3 protein.

333 We next determined whether CPEB3 regulated GluA1 expression during stress. CPEB3 knockout mice
334 were exposed to predator odor and the GluA1 expression level in the cerebellar cortex was quantified
335 24 hrs later. The intensity of GluA1 staining in the molecular layer in lobule 5 in naive CPEB3 knockout
336 mice was not different from wild-type littermates ($GluA1_{CPEB3-KO}/GluA1_{WT}$:0.95±0.22; unpaired t-test: $t(2)$
337 $= 0.4$, $p=0.708$; Figure 5B). There was also no difference in the level of GluA1-ir in the somatic layer (KO:
338 1.18±0.23; unpaired t-test: $t(2) = -1.40$, $p=0.234$). However stress no longer reduced GluA1-ir in the
339 molecular layer in CPEB3 KO mice (stressed: 1.06±0.07; unpaired t-test: $t(6) = -0.81$, $p=0.449$; Figure 5C).
340 No difference was found in GluA1-ir in the somatic (or Purkinje cell) layer in naive and stressed CPEB3
341 KO mice (stress: 0.96±0.04; unpaired t-test: $t(6) = 1.92$, $p=0.103$). In contrast to KO mice, emotional
342 stress reduced GluA1-ir in the molecular layer in lobule 5 by 16 ± 4% (WT vs KO; unpaired t-test: $t(5) = -$
343 3.40, $p=0.019$) in wild-type mice (Figure 5C). These results indicate that CPEB3 is required for the stress-
344 induced decrease in GluA1 expression in Bergmann glial cells.

345 To determine if these effects were associated with a change in the functional expression of AMPA
346 receptors we stimulated parallel fibers and quantified the evoked AMPA currents in Bergmann glial cells
347 from naïve CPEB3 knockout mice. NBQX application blocked 37.5% of the parallel fiber-evoked current
348 (Fig 6), which was indistinguishable from recordings in naïve WT mice. Thus deletion of CPEB3 did not
349 alter basal AMPA receptor expression in Bergmann glial cells. We next determined whether knockout of
350 CPEB3 prevented the stress-induced decrease in AMPAR currents in astrocytes. Mutant mice were
351 exposed to fox urine, and the amplitude of the parallel fiber-evoked currents were determined the next
352 day. When NBQX was applied the inward current was reduced by 34.6%, and this inhibition is
353 comparable to naïve KO mice (unpaired t-test: $t(8) = 0.56$, $p = 0.59$), indicating that stress no longer
354 reduced AMPAR expression in Bergmann glial cells in CPEB3 KO mice. Therefore, CPEB3 is required for
355 the stress-induced decrease in the level of GluA1 and AMPA receptors in cerebellar astrocytes following
356 stress, but is not required for their basal expression.

357 **A β-adrenergic receptor-adenylyl cyclase 5 pathway mediates the stress-induced decrease in GluA1**

358 Emotional stress triggers the release of norepinephrine in the cerebellum and alters synaptic
359 transmission between cerebellar neurons (Siggins et al., 1971; Kondo and Marty, 1998; Liu et al., 2010;
360 Paukert et al., 2014). We used a pharmacological approach to determine whether the release of
361 norepinephrine was involved in the stress-induced change in GluA1 expression. Age matched littermates
362 were divided into three groups: naive control, administration of propranolol (20 mg/kg i.p.), a beta
363 adrenergic blocker, 30 minutes before the predator odor exposure, and saline injection 30 minutes prior
364 to the predator odor exposure. As expected, GluA1-ir in lobule 5 was reduced by 26 ± 2% following fox
365 urine exposure (naive n=5; stress n=5). However after propranolol administration, stress produced a
366 smaller reduction in the levels of GluA1-ir (12 ± 1%, n= 5; Fig 7), compared to naive control mice (stress-
367 induced change relative to naive control: vehicle vs propranolol, the molecular layer, unpaired t-test:

JNeurosci Accepted Manuscript

368 t(8) = -4.57, p=0.002; Bergmann glial cell somata, t-test: t(8) = 1.07, p=0.32; Fig 7). Because propranolol
369 and saline injection did not suppress GluA1 expression in naïve mice (molecular layer: saline/naïve = 114
370 ± 10%; propranolol/naïve = 97 ± 13%; unpaired t-test: t(4)= 0.68739, p = 0.53; Bergmann glial layer:
371 saline/naïve = 94 + 15%; propranolol/naïve = 108 + 18%; t(4) = -0.56609; P = 0.60), propranolol partially
372 prevented the stress-induced decrease in GluA1 immunoreactivity. This suggests that norepinephrine
373 released during stress activates β-adrenergic receptors, leading to a reduction in GluA1 expression in
374 Bergmann glial cells. Because the level of GluA1-ir in stressed mice that were injected with propranolol
375 remained lower than in naive controls (Figure 7), additional signaling pathways or stress hormones may
376 also contribute to the downregulation of GluA1 expression in Bergmann glial cells.

377 β-adrenergic receptors are coupled to adenylyl cyclases and activation of these receptors increases
378 cAMP levels in astrocytes (Rougon et al., 1983). Therefore stress may activate adenylyl cyclase in
379 Bergmann glial cells and reduce GluA1 expression. We detected AC5/6-immunoreactivity in the
380 molecular layer, and this was co-localized with GFAP-ir (Figure 8A). Control experiments showed that
381 AC5/6 staining was reduced in AC5 KO mice (Figure 8A). We next tested whether deletion of AC5
382 prevented the stress-induced decrease in GluA1 expression. Exposure to fox urine reduced the level of
383 GluA1-ir in lobule 5 in the molecular layer in wild-type mice (WT stress: 0.89±0.06; unpaired t-test: t(6) =
384 2.88, p=0.031, Fig 8B) as well as in the somatic layer (stress: 0.88±0.06; unpaired t-test: t(6) = 2.63,
385 p=0.036). The stress-induced decrease in GluA1-ir in both molecular and Purkinje cell layers was
386 abolished in AC5 knockout mice (Fig 8C; in the molecular layer, KO stress: 1.08±0.18, unpaired t-test: t(2)
387 = -0.75, p=0.494; in the PC layer, KO stress: 0.93±0.09, t(2) = 1.32, p=0.256). These results indicate that
388 the stress-induced downregulation of GluA1 expression requires AC5 activation.

389

390

JNeurosci Accepted Manuscript

391 **DISCUSSION**

392 AMPA receptors are found in most neurons in the CNS and mediate excitatory synaptic transmission.
393 Neuronal activity can regulate the expression and activity of synaptic AMPA receptors (Wang et al.,
394 2010), modifying synaptic efficacy and leading to experience-dependent changes in behavior. While the
395 critical role of neuronal AMPARs in synaptic plasticity is well established, these receptors are also
396 expressed in astrocytes. In the cerebellum, Bergmann glial cells express GluA1 and GluA4 subunits and
397 thus have Ca permeable AMPA receptors (Piet and Jahr, 2007). Genetic knockdown of GluA1 subunits or
398 transgenic expression of GluA2 in Bergmann glial cells reduces the length of their processes (Saab et al.,
399 2012; Iino et al., 2001). These changes lead to an impairment of motor coordination (Saab et al., 2012)
400 and suggest that the activation of GluA1-containing AMPA receptors in astrocytes controls both their
401 morphology and cerebellar-dependent behavioral output. Consequently, an activity-dependent change
402 in astrocyte GluA1 expression is expected to alter astrocyte morphology. In this study we demonstrate
403 that predator odor stress causes retraction of the lateral processes and lowers GluA1 expression in
404 Bergmann glial cells. We further identified the underlying mechanisms and show that stress triggers
405 norepinephrine release, activation of adrenergic receptors and AC5, and induces a CPEB3-dependent
406 suppression of GluA1 expression.

407 *Regulation of glial GluA1 via CPEB3*. Stress can increase GluA2 gene transcription expression and
408 potentiate GluA1 phosphorylation and this has been shown to reduce the threshold for LTP in neurons
409 in several brain regions (Hu et al., 2007; Liu et al., 2010; Vialou et al., 2010; Lee et al., 2013; Li et al.,
410 2014; Perusini et al., 2016). In contrast, our results show that stress reduces GluA1 expression in
411 astrocytes. CPEB3, a GluA1 mRNA binding protein, produces a bi-directional regulation of GluA1 protein
412 synthesis in neurons, as mono-ubiquitination of CPEB3 enhances protein synthesis, whereas sumoylated
413 CPEB3 suppresses translation (Pavlopoulos et al., 2011; Drisaldi et al., 2015). Genetic deletion of CPEB3
414 attenuates a learning-induced increase in AMPA receptor expression in hippocampal neurons, and
415 impairs spatial memory formation and contextual fear learning (Pavlopoulos et al., 2011; Chao et al.,
416 2013; Fioriti et al., 2015). Although CPEB3 is expressed at high levels in neurons, it is also present in
417 astrocytes, including cerebellar Bergmann glial cells. Our finding that deletion of CPEB3 prevented a
418 stress-induced decrease in GluA1-ir and the amplitude of AMPAR currents suggests that CPEB3 is
419 required for the reduction in GluA1 levels in Bergmann glial cells following acute emotional stress. These
420 results can be explained by a simple model, in which a stress-induced binding of CPEB3 to GluA1 mRNA
421 suppresses GluA1 synthesis in astrocytes.

422 A decrease in GluA1 protein expression level could result from reduced synthesis or/and accelerated
423 degradation. While the GluA1 degradation rate in Bergmann glial cells has not been characterized, a
424 study using HEK cells showed that in the presence of a protein synthesis inhibitor, GluA1 expression
425 decreased by 30% in 3 hrs (Huo et al., 2015), suggesting that GluA1 degradation can occur rapidly . Our
426 finding that deletion of CPEB3 prevented the reduction in GluA1 expression is consistent with a model in
427 which stress suppresses GluA1 synthesis, such that protein degradation controls GluA1 levels, leading to
428 GluA1 decrease. Stress may also enhance GluA1 degradation as shown following neuronal activity
429 (Widagdo et al., 2015) but this remains to be tested.

JNeurosci Accepted Manuscript

430 In addition to Bergmann glial cells, CPEB3 is also expressed at a high level in the molecular layer
431 interneurons (Fig 5) and regulates synaptic GluA2 expression (Savtchouk et al., 2016). A number of
432 CPEB3 targets have been identified and thus deletion of CPEB3 is likely to increase the expression of
433 these target proteins, including the scaffolding protein PSD95 and NMDA receptors, as shown in the
434 hippocampal neurons (Chao et al., 2013; Huang et al., 2014). Since GluA1 expression in Bergmann glial
435 cells can also be regulated indirectly by sonic hedgehog derived from Purkinje cells (Farmer et al., 2016),
436 deletion of CPEB3 in interneurons may alter neuron-astrocyte signaling, and thereby regulate GluA1
437 expression in astrocytes. Our results show that deletion of CPEB3 did not alter AMPA receptor-mediated
438 currents and GluA1-ir relative to wildtype naïve animals (Figs 3 and 4). It is therefore unlikely that CPEB3
439 expression in interneurons is required to sustain the GluA1 level in Bergmann glial cells. It remains to be
440 tested whether neuronal CPEB3 mediates neuron-astrocyte signaling during stress and triggers the
441 decrease in GluA1 in Bergmann glial cells.

442 *β-adrenergic receptor-adenylyl cyclase 5 signaling pathways in astrocytes*. Astrocytes in the cerebellum
443 and other brain regions express adrenergic (Porter and McCarthy, 1997) and glucocorticoid receptors
444 (Porter and McCarthy, 1997) allowing them to directly respond to stress hormones. Noradrenaline in
445 particular can modulate astrocyte structure and function, as β-adrenergic agonists increase the levels of
446 cyclic AMP in purified glial cells and induce rapid morphological changes. Conversely α-adrenoceptor
447 antagonists inhibit the activation of astrocyte networks that are triggered by arousal and activation of
448 the locus coeruleus (Rougon et al., 1983; Vardjan et al., 2014; Paukert et al., 2014; Ding et al., 2013).

449 Neurons in the locus coeruleus innervate the cerebellum, and noradrenaline release increases inhibitory
450 interneuron activity and reduces Purkinje cell spiking (Siggins et al., 1971). We have previously shown
451 that fox urine exposure induced a lasting change in GluA2 expression in cerebellar stellate cells *via* the
452 activation of β-adrenergic receptors (Liu et al., 2010a). Paukert et al. (2014) demonstrated a Ca^{2+} rise in
453 cerebellar Bergmann glial cells upon arousal and this was mediated by adrenergic receptors. Together
454 these studies strongly suggest that predator odor stress can elevate noradrenaline levels and initiate
455 noradrenergic signaling in cerebellar Bergmann glial cells. In this study, we identified a molecular
456 cascade that orchestrates stress-induced astrocyte plasticity in the cerebellum. We show that the stress-
457 induced decrease in GluA1-ir levels in Bergmann glial cells was partially prevented by prior
458 administration of a β-adrenergic receptor antagonist. Therefore, activation of adrenergic receptors
459 during acute stress induces long-lasting astrocyte plasticity in the cerebellum. β-adrenergic receptors
460 are coupled to adenylyl cyclases and genetic deletion of adenylyl cyclase subtypes show that they are
461 critically involved in anxiety-like behaviors (Krishnan et al., 2008). AC5 KO mice exhibit anxiolytic and
462 antidepressant phenotypes in behavioral assays, and show a reduced stress-coping ability (Kim et al.,
463 2008; Krishnan et al., 2008; Kim and Han, 2009). We found that Bergmann glial cells express AC5 and its
464 deletion prevents the suppression of GluA1 levels following acute predator odor exposure. Thus, AC5-
465 dependent astrocyte plasticity may contribute to the stress response and the change in behavior in AC5
466 KO mice. However, we cannot rule out the possibility that the presence of AC5 in cerebellar neurons
467 may indirectly modulate GluA1 levels in Bergmann glial cells during stress. Because knockdown of GluA1
468 in Bergmann glial cells reduces the length of fine processes, we propose that regulation of GluA1

JNeurosci Accepted Manuscript

469 expression is the molecular event that links a physiological stimulus to the subsequent structural
470 remodeling of astrocytic structure.

471 *Functional consequences of astrocyte plasticity*. The fine processes of Bergmann glial cells form close
472 contacts with both excitatory and inhibitory synapses in the molecular layer of the cerebellar cortex
473 (Ango et al., 2008). Because the glial glutamate transporter, GLAST, clears glutamate after release
474 (Chaudhry et al., 1995; Clark and Cull-Candy, 2002), a retraction of astrocyte fine processes could
475 enhance glutamate transmission by removing glutamate transporters from the synapses. Bergmann glial
476 cells also express GABA transporters (Barakat and Bordey, 2002), and thus retraction of glial processes
477 may also facilitate inhibitory transmission. Conversely the neurotransmitters, glutamate and GABA, alter
478 the activity of Bergmann glial cells *via* the activation of astrocytic AMPA and GABA receptors (Müller et
479 al., 1994; Clark and Barbour, 1997). Since parallel fiber stimulation activates Ca^{2+} permeable GluA1-
480 containing receptors in Bergmann glial cells, acute stress will reduce Ca^{2+} entry through AMPA receptors
481 which in turn can gate the release of glutamate from Bergmann glial cells (Cervetto et al., 2015).
482 Therefore, stress may reduce the release of gliotransmitters and attenuate bidirectional signaling
483 between neurons and glial cells.

484 The cerebellum is involved in motor-coordination but has additional non-motor functions which are well
485 documented in humans (Schmahmann et al., 2007). The best characterized cerebellar non-motor role in
486 rodents is the consolidation of fear memory and social interaction (Sacchetti et al., 2002b; Carta et al.,
487 2019). Fear conditioning selectively enhances excitatory and inhibitory synaptic transmission in lobule 5,
488 a lobule that is critically involved in fear memory consolidation (Sacchetti et al., 2002, 2004; Scelfo et al.,
489 2008; Ruediger et al., 2011). Thus the stress-induced retraction of glial process in cerebellar lobule 5 is
490 likely to increase synaptic transmission and may serve as a mechanism for a stress-enhanced memory
491 consolidation (Bowers and Ressler, 2015; Perusini et al., 2016; Bender et al., 2018b, 2018a).

492 Deletion of GluA1/GluA4 from all BG cells shows that their expression optimizes motor function (Saab et
493 al., 2012). Because cerebellar vermal lobule 5B-8B receives input from the cerebral motor cortex, and is
494 involved in controlling posture and locomotion in macaques (Coffman et al., 2011), the stress-induced
495 reduction in GluA1 and retraction of BG processes in lobule 5 may similarly influence motor
496 coordination. For example, episodic ataxia type 1 results from increased GABA release onto Purkinje
497 cells (Herson et al., 2003) and these episodes can be precipitated by emotional stress (Jen, 2000). A
498 stress-induced remodeling of glial cell processes may enhance inhibitory transmission, and contribute to
499 motor deficits in episodic ataxia (Wulff et al., 2007).

500 AMPARs in Bergmann glial cells are known to control astrocyte structure, and we show that GluA1
501 expression can undergo an experience-dependent change. The activity-dependent regulation of GluA1
502 may serve as a common mechanism for structural remodeling of astrocytes in other brain regions as
503 astrocytes in the olfactory bulb also express GluA1 and Ca^{2+} permeable AMPA receptors (Droste et al.,
504 2017). Our findings that acute emotional stress regulates the expression of GluA1 via an adrenergic
505 receptor/AC5/CPEB3 pathway reveals a novel mechanism underlying glial plasticity.

506

507

JNeurosci Accepted Manuscript

508 **FIGURE LEGENDS**

509 **Figure 1. Bergmann glial cell lateral processes are shorter after stress**
510 **A.** Confocal images showing that GFP::NPY mice exhibit fluorescent labeling of a subset of GFAP positive
511 Bergmann glial cells. **B.** Retraction of the lateral processes of Bergmann glial cells was evident 3hrs after
512 exposure to fox urine and the effect became more pronounced at 24 hours. Upper panels show whole
513 cell images and each was made from a z projection of all 25-30 confocal slices. Inserts illustrate z
514 projections of 2 to 3 consecutive confocal slices to reveal individual processes. **C.** Cumulative
515 distribution of the length of lateral processes in Bergmann glial cells from naïve mice, and 3 and 24
516 hours after stress exposure (836-914 processes from 22-24 cells/each condition; N = 7). **D.** Top,
517 schematic representation of the experimental design. Bottom, sagittal section of the cerebellum from an
518 GFAP-GFP mouse showing the lobules and areas analyzed in this study (lobules 5 and 9). ML: Molecular
519 layer, PL: Purkinje cell layer. Scale bar 20 µm. *, p<0.0001; **, p<0.000001 (Kolmogorov Smirnov test).

520

521 **Figure 2**. **Stress reduces GluA1 expression in Bergmann glial cell processes in cerebellar lobule 5**
522 **A.** Confocal images of cerebellar cortex stained for the GluA1 AMPA receptor subunit in GFAP-GFP mice
523 shows that GluA1 is highly expressed in Bergmann glial cells. **B.** *Top:* Epifluorescence GluA1-ir images of
524 lobule 5 in a naive control mice and after stress. *Bottom*: the mean intensity of GluA1 immunoreactivity
525 (ir) in Bergmann cell processes (in the molecular layer of the cerebellar cortex) and the somata of
526 Bergmann cells (located in the Purkinje cell layer) in lobule 5. Stress reduced the level of GluA1-ir in the
527 molecular layer (naive N=6, stress N=6). **C.** *Top:* GluA1-ir images of lobule 9. *Bottom*: Mean GluA1-ir in
528 Bergmann processes and somata in cerebellar lobule 9. ML: Molecular layer, GL: Granule cell layer, PL:
529 Purkinje cell layer, ns: not significant. Scale bars 50 µm (A), 100 µm (B). *, p<0.02 (unpaired t-test)

530 **Figure 3**. **Predator odor stress induced a rapid decrease in GluA1-ir in cerebellar lobule 5**
531 **A-B.** GluA1-ir in lobule 5 decreased 3 hrs after exposure to fox urine. **C**. Quantification of GluA1-ir in the
532 molecular layer of each lobule (lobules 1-10) showing a lack of effect of stress on GluA1 expression in
533 lobules 1-3 and 7-10 (naïve N=4; stress N=4). **D**. A reduction in GluA1-ir in lobule 5 was detected as early
534 as 3 hr, and lasted for at least 24 hrs, after stress. *, p < 0.04 (unpaired t-test)

535

536 **Figure 4. Exposure to predator odor decreased AMPAR-mediated currents in Bergmann glial cells.**
537 Cerebellar slices were prepared from the vermis of naive animals or stressed mice (24 hr after fox urine
538 exposure). Stimulation of parallel fibers evoked an inward current in Bergmann glial cells located in
539 cerebellar lobule 5. Application of NBQX (10 µM) inhibits AMPA receptor-mediated currents. **A.** Example
540 current traces in the presence and absence of NBQX (left) and corresponding time course of the evoked
541 AMPAR-mediated current amplitude (right). **B.** Summary data of the change in current amplitude over
542 time (naïve N=6; stress N=6). **C.** Average current ratio (=I_{NBQX} / I_{total}) shows a decrease after stress relative
543 to control. *, p < 0.005 (unpaired t-test).

544

545 **Figure 5. Deletion of CPEB3 prevents the stress-induced reduction in GluA1 expression in Bergmann**
546 **glial cells**

JNeurosci Accepted Manuscript

547 **A.** Confocal images of GFAP- and CPEB3-ir indicate that CPEB3 is expressed in Bergmann glial cell
548 processes (upper right corner) as well as in granule cells and molecular layer interneurons. CPEB3-ir was
549 absent in CPEB3 KO mice. **B.** Epifluorescence images, and the corresponding quantification of GluA1-ir in
550 wild type and CPEB3 knockout mice, indicates that there is no difference between genotypes (WT N=3,
551 KO N=3). **C.** Epifluorescence images and GluA1-ir in naive KO and stressed KO mice. Deletion of CPEB3
552 did not alter GluA1-ir in the molecular layer (naive KO N=4, stress KO N=4). Stress reduced GluA1-ir by
553 16 ± 4% in wild-type mice (naive WT N=3, stress WT N=3).
554 ML: Molecular layer, GL: Granule cell layer, PL: Purkinje cell layer. Scale bars 50 µm (A), 100 µm (B-C). *,
555 $p < 0.02$ (unpaired t-test).
556
557 **Figure 6. Stress failed to reduce AMPAR-mediated currents in Bergmann glial cells in CPEB3 KO mice**
558 Cerebellar slices were prepared 24 hr after fox urine exposure or from naïve CPEB3 knockout mice.
559 Stimulation of parallel fibers evoked an inward current in Bergmann glial cells and application of NBQX
560 was used to assess the contribution of AMPARs to the total evoked current. **A.** Example current traces
561 (left) and corresponding time course of the change in current amplitude (right). **B.** Summary data of
562 current amplitude over time (naïve N=5; stress N=5). **C.** Average current ratio (I_{NBQX} / I_{total}) remains
563 unaltered after stress relative to control.
564
565 **Figure 7. Stress-induced decrease in GluA1-ir is prevented by a βadrenergic receptor antagonist**
566 **A.** The downregulation of GluA1-ir after stress was partially prevented by propranolol administration. **B.**
567 Quantification of GluA1-ir in the molecular layer of lobule 5 from animals administered saline or
568 propranolol prior to stress (naive N=5, saline N=5, propranolol N=5). The level of GluA1-ir was
569 significantly higher in the molecular layer in the propranolol-administered animals compared to the
570 saline-injected mice. Scale Bar 100 µm. *, $p<0.002$ (unpaired t-test).
571
572 **Figure 8. Adenylyl cyclase 5 mediates the stress-induced decrease in GluA1 expression**
573 **A.** Double staining for GFAP and adenylyl cyclase 5 (AC5) indicates that AC5 is expressed in the processes
574 of Bergmann glial cells. AC5-ir was reduced in AC5 knockout mice. **B.** Epifluorescence images and the
575 corresponding quantification of GluA1-ir in naive wild type animals and after stress (BG processes, naive
576 N=4, stress N=4). **C.** In contrast, AC5 knockout mice no longer showed any decrease in GluA1-ir after
577 stress (naive-KO N=3, stress-KO N=3). ML: Molecular layer, GL: Granule cell layer, PL: Purkinje cell layer.
578 Scale bars 50 µm (A), 100 µm (B-C). *, $p<0.04$ (unpaired t-test).
579
580
581
582

JNeurosci Accepted Manuscript

583 REFERENCES

584 Ango F, Wu C, Van Der Want JJ, Wu P, Schachner M, Huang ZJ (2008) Bergmann glia and the recognition
585 molecule CHL1 organize GABAergic axons and direct innervation of Purkinje cell dendrites Ghosh A,
586 ed. PLoSBiol 6:739–756.

587 Araque A, Parpura V, Sanzgiri RP, Haydon PG (1999) Tripartite synapses: glia, the unacknowledged
588 partner. Trends Neurosci 22:208–215.

589 Arganda-Carreras I, Fernández-González R, Muñoz-Barrutia A, Ortiz-De-Solorzano C (2010) 3D
590 reconstruction of histological sections: Application to mammary gland tissue. Microsc Res Tech
591 73:1019–1029.

592 Barakat L, Bordey A (2002) GAT-1 and reversible GABA transport in Bergmann glia in slices. J
593 Neurophysiol 88:1407–1419.

594 Baude A, Molnar E, Latawiec D, McIlhinney RAJ, Somogyi P (1994) Synaptic and nonsynaptic localization
595 of the GluR1 subunit of the AMPA- type excitatory amino acid receptor in the rat cerebellum. J
596 Neurosci 14:2830–2843.

597 Bender CL, Calfa GD, Molina VA (2016) Astrocyte plasticity induced by emotional stress: A new partner
598 in psychiatric physiopathology? Prog Neuro-Psychopharmacology Biol Psychiatry 65:68–77.

599 Bender CL, Giachero M, Comas-Mutis R, Molina VA, Calfa GD (2018a) Stress influences the dynamics of
600 hippocampal structural remodeling associated with fear memory extinction. Neurobiol Learn Mem
601 155:412–421

602 Bender CL, Otamendi A, Calfa GD, Molina VA (2018b) Prior stress promotes the generalization of
603 contextual fear memories: Involvement of the gabaergic signaling within the basolateral amygdala
604 complex. Prog Neuro-Psychopharmacology Biol Psychiatry 83:18–26

605 Bostan AC, Dum RP, Strick PL (2013) Cerebellar networks with the cerebral cortex and basal ganglia.
606 Trends CognSci 17:241–254.

607 Bowers ME, Ressler KJ (2015) An Overview of Translationally Informed Treatments for Posttraumatic
608 Stress Disorder: Animal Models of Pavlovian Fear Conditioning to Human Clinical Trials. Biol
609 Psychiatry 78:E15–E27

610 Carta I, Chen CH, Schott AL, Dorizan S, Khodakhah K (2019) Cerebellar modulation of the reward circuitry
611 and social behavior. Science 363:eaav0581

612 Cervetto C, Frattaroli D, Venturini A, Passalacqua M, Nobile M, Alloisio S, Tacchetti C, Maura G, Agnati
613 LF, Marcoli M (2015) Calcium-permeable AMPA receptors trigger vesicular glutamate release from
614 Bergmann gliosomes. Neuropharmacology 99:396–407.

615 Chao H-W, Tsai L-Y, Lu Y-L, Lin P-Y, Huang W-H, Chou H-J, Lu W-H, Lin H-C, Lee P-T, Huang Y-S (2013)
616 Deletion of CPEB3 Enhances Hippocampus-Dependent Memory via Increasing Expressions of
617 PSD95 and NMDA Receptors. J Neurosci 33:17008–17022.

618 Chaudhry FA, Lehre KP, LookerenCampagne M van, Ottersen OP, Danbolt NC, Storm-Mathisen J (1995)
619 Glutamate transporters in glial plasma membranes: Highly differentiated localizations revealed by

JNeurosci Accepted Manuscript

620 quantitative ultrastructural immunocytochemistry. Neuron 15:711–720.

621 Christoffel DJ, Golden SA, Russo SJ (2011) Structural and synaptic plasticity in stress-related disorders.
622 Rev Neurosci 22:535–549.

623 Clark BA, Barbour B (1997) Currents evoked in Bergmann glial cells by parallel fibre stimulation in rat
624 cerebellar slices. J Physiol 502 (Pt 2):335–350.

625 Clark BA, Cull-Candy SG (2002) Activity-dependent recruitment of extrasynaptic NMDA receptor
626 activation at an AMPA receptor-only synapse. J Neurosci 22:4428–4436.

627 Coffman KA, Dum RP, Strick PL (2011) Cerebellar vermis is a target of projections from the motor areas
628 in the cerebral cortex. Proc Natl Acad Sci 108:16068–16073

629 Davidson RJ, McEwen BS (2012) Social influences on neuroplasticity: stress and interventions to promote
630 well-being. Nat Neurosci 15:689–695.

631 De Zeeuw CI, Hoogland TM (2015) Reappraisal of Bergmann glial cells as modulators of cerebellar circuit
632 function. Front Cell Neurosci 9:246.

633 De Zeeuw CI, Ten Brinke MM (2015) Motor learning and the cerebellum. Cold Spring HarbPerspectBiol
634 7:a021683.

635 Ding F, O'Donnell J, Thrane AS, Zeppenfeld D, Kang H, Xie L, Wang F, Nedergaard M (2013) α1-
636 Adrenergic receptors mediate coordinated Ca2+ signaling of cortical astrocytes in awake, behaving
637 mice. Cell Calcium 54:387–394.

638 Drisaldi B, Colnaghi L, Fioriti L, Rao N, Myers C, Snyder AM, Metzger DJ, Tarasoff J, Konstantinov E, Fraser
639 PE, Manley JL, Kandel ER (2015) SUMOylation Is an Inhibitory Constraint that Regulates the Prion-
640 like Aggregation and Activity of CPEB3. Cell Rep 11:1694–1702.

641 Droste D, Seifert G, Seddar L, Jädtke O, Steinhäuser C, Lohr C (2017) Ca(2+)-permeable AMPA receptors
642 in mouse olfactory bulb astrocytes. Sci Rep 7:44817.

643 Edwards S, Baynes BB, Carmichael CY, Zamora-Martinez ER, Barrus M, Koob GF, Gilpin NW (2013)
644 Traumatic stress reactivity promotes excessive alcohol drinking and alters the balance of prefrontal
645 cortex-amygdala activity. Transl Psychiatry 3:e296.

646 Farmer WT, Abrahamsson T, Chierzi S, Lui C, Zaelzer C, Jones E V., Bally BP, Chen GG, Théroux JF, Peng J,
647 Bourque CW, Charron F, Ernst C, Sjóström PJ, Murai KK (2016) Neurons diversify astrocytes in the
648 adult brain through sonic hedgehog signaling. Science 351:849–854.

649 Fioriti L, Myers C, Huang Y-Y, Li X, Stephan JS, Trifilieff P, Colnaghi L, Kosmidis S, Drisaldi B, Pavlopoulos
650 E, Kandel ER (2015) The Persistence of Hippocampal-Based Memory Requires Protein Synthesis
651 Mediated by the Prion-like Protein CPEB3. Neuron 86:1433–1448.

652 Fischer H, Andersson JL, Furmark T, Fredrikson M (2000) Fear conditioning and brain activity: a positron
653 emission tomography study in humans. BehavNeurosci 114:671–680.

654 Franklin TB, Saab BJ, Mansuy IM (2012) Neural Mechanisms of Stress Resilience and Vulnerability.
655 Neuron 75:747–761.

JNeurosci Accepted Manuscript

656 Herson PS, Virk M, Rustay NR, Bond CT, Crabbe JC, Adelman JP, Maylie J (2003) A mouse model of
657 episodic ataxia type-1. Nat Neurosci 6:378–383.

658 Hu H, Real E, Takamiya K, Kang M-G, Ledoux J, Huganir RL, Malinow R (2007) Emotion enhances learning
659 via norepinephrine regulation of AMPA-receptor trafficking. Cell 131:160–173.

660 Huang WH, Chao HW, Tsai LY, Chung MH, Huang YS (2014) Elevated activation of CaMKIIα in the CPEB3-
661 knockout hippocampus impairs a specific form of NMDAR-dependent synaptic depotentiation.
662 Front Cell Neurosci 8:367.

663 Huo Y, Khatri N, Hou Q, Gilbert J, Wang G, Man HY (2015) The deubiquitinating enzyme USP46 regulates
664 AMPA receptor ubiquitination and trafficking. J Neurochem 134:1067–1080

665 Iino M, Goto K, Kakegawa W, Okado H, Sudo M, Ishiuchi S, Miwa A, Takayasu Y, Saito I, Tsuzuki K, Ozawa
666 S (2001) Glia-synapse interaction through Ca2+-permeable AMPA receptors in Bergmann glia.
667 Science 292:926–929.

668 Jen J (2000) Familial Episodic Ataxias and related ion channel disorders. Curr Treat Options Neurol
669 2:429–431.

670 Kim K-S, Han P-L (2009) Mice lacking adenylyl cyclase-5 cope badly with repeated restraint stress. J
671 Neurosci Res 87:2983–2993.

672 Kim K-S, Lee K-W, Baek I-S, Lim C-M, Krishnan V, Lee J-K, Nestler EJ, Han P-L (2008) Adenylyl cyclase-5
673 activity in the nucleus accumbens regulates anxiety-related behavior. J Neurochem 107:105–115.

674 Kondo S, Marty A (1998) Differential effects of noradrenaline on evoked, spontaneous and miniature
675 IPSCs in rat cerebellar stellate cells. J Physiol 509 (Pt 1):233–243.

676 Krishnan V, Graham A, Mazei-Robison MS, Lagace DC, Kim K-S, Birnbaum S, Eisch AJ, Han P-L, Storm DR,
677 Zachariou V, Nestler EJ (2008) Calcium-Sensitive Adenylyl Cyclases in Depression and Anxiety:
678 Behavioral and Biochemical Consequences of Isoform Targeting. Biol Psychiatry 64:336–343.

679 Lee S, Song B, Kim J, Park K, Hong I, An B, Song S, Lee J, Park S, Kim J, Park D, Lee CJ, Kim K, Shin KS, Tsien
680 RW, Choi S (2013) GluA1 phosphorylation at serine 831 in the lateral amygdala is required for fear
681 renewal. Nat Neurosci 16:1436–1444.

682 Li C, Yang Y, Liu S, Fang H, Zhang Y, Furmanski O, Skinner J, Xing Y, Johns RA, Huganir RL, Tao F (2014)
683 Stress Induces Pain Transition by Potentiation of AMPA Receptor Phosphorylation. J Neurosci
684 34:13737–13746.

685 Liu Y, Formisano L, Savtchouk I, Takayasu Y, Szabó G, Zukin RS, Liu SJ (2010) A single fear-inducing
686 stimulus induces a transcription-dependent switch in synaptic AMPAR phenotype. Nat Neurosci
687 13:223–231.

688 McEwen BS, Gianaros PJ (2010) Central role of the brain in stress and adaptation: links to socioeconomic
689 status, health, and disease. Ann N Y AcadSci 1186:190–222.

690 Mobley PL, Combs DL (1992) Norepinephrine-mediated protein phosphorylation in astrocytes. Brain Res
691 Bull 29:289–295.

692 Müller T, Fritschy JM, Grosche J, Pratt GD, Möhler H, Kettenmann H (1994) Developmental regulation of

JNeurosci Accepted Manuscript

693 voltage-gated K+ channel and GABAA receptor expression in Bergmann glial cells. J Neurosci
694 14:2503–2514.

695 Papp M, Gruca P, Lason-Tyburkiewicz M, Litwa E, Willner P (2014) Effects of chronic mild stress on the
696 development of drug dependence in rats. BehavPharmacol 25:1.

697 Paukert M, Agarwal A, Cha J, Doze VA, Kang JU, Bergles DE (2014) Norepinephrine controls astroglial
698 responsiveness to local circuit activity. Neuron 82:1263–1270.

699 Pavlopoulos E, Trifilieff P, Chevaleyre V, Fioriti L, Zairis S, Pagano A, Malleret G, Kandel ER (2011)
700 Neuralized1 activates CPEB3: a function for nonproteolytic ubiquitin in synaptic plasticity and
701 memory storage. Cell 147:1369–1383.

702 Paxinos G, Franklin K (2001) The Mouse Brain in Stereotaxic Coordinates. Second edition, San Diego
703 Academic Press.

704 Perusini JN, Meyer EM, Long VA, Rau V, Nocera N, Avershal J, Maksymetz J, Spigelman I, Fanselow MS
705 (2016) Induction and Expression of Fear Sensitization Caused by Acute Traumatic Stress.
706 Neuropsychopharmacology 41:45–57.

707 Petralia RS, Wenthold RJ (1992) Light and electron immunocytochemical localization of AMPA-selective
708 glutamate receptors in the rat brain. J Comp Neurol 318:329–354.

709 Piet R, Jahr CE (2007) Glutamatergic and Purinergic Receptor-Mediated Calcium Transients in Bergmann
710 Glial Cells. J Neurosci 27:4027–4035.

711 Porter JT, McCarthy KD (1997) Astrocytic neurotransmitter receptors in situ and in vivo. ProgNeurobiol
712 51:439–455.

713 Rougon G, Noble M, Mudge AW (1983) Neuropeptides modulate the beta-adrenergic response of
714 purified astrocytes in vitro. Nature 305:715–717.

715 Ruediger S, Vittori C, Bednarek E, Genoud C, Strata P, Sacchetti B, Caroni P (2011) Learning-related
716 feedforward inhibitory connectivity growth required for memory precision. Nature 473:514–518.

717 Saab AS, Neumeyer A, Jahn HM, Cupido A, Šimek AAM, Boele H-J, Scheller A, Le Meur K, Götz M, Monyer
718 H, Sprengel R, Rubio ME, Deitmer JW, De Zeeuw CI, Kirchhoff F (2012) Bergmann glial AMPA
719 receptors are required for fine motor coordination. Science 337:749–753.

720 Sacchetti B, Baldi E, Lorenzini CA, Bucherelli C (2002) Cerebellar role in fear-conditioning consolidation.
721 Proc Natl AcadSci U S A 99:8406–8411.

722 Sacchetti B, Scelfo B, Tempia F, Strata P (2004) Long-term synaptic changes induced in the cerebellar
723 cortex by fear conditioning. Neuron 42:973–982.

724 Savtchouk I, Liu SJ (2011) Remodeling of synaptic AMPA receptor subtype alters the probability and
725 pattern of action potential firing. J Neurosci 31:501–511.

726 Savtchouk I, Sun L, Bender CL, Yang Q, Szabó G, Gasparini S, Liu SJ (2016) Topological Regulation of
727 Synaptic AMPA Receptor Expression by the RNA-Binding Protein CPEB3. Cell Rep 17:86–103.

728 Scelfo B, Sacchetti B, Strata P (2008) Learning-related long-term potentiation of inhibitory synapses in

JNeurosci Accepted Manuscript

729 the cerebellar cortex. Proc Natl AcadSci U S A 105:769–774.

730 Schmahmann JD, Weilburg JB, Sherman JC (2007) The neuropsychiatry of the cerebellum - insights from
731 the clinic. The Cerebellum 6:254–267

732 Shin LM, Liberzon I (2010) The neurocircuitry of fear, stress, and anxiety disorders.
733 Neuropsychopharmacology 35:169–191.

734 Siggins GR, Hoffer BJ, Oliver AP, Bloom FE (1971) Activation of a central noradrenergic projection to
735 cerebellum. Nature 233:481–483.

736 Staples LG (2010) Predator odor avoidance as a rodent model of anxiety: learning-mediated
737 consequences beyond the initial exposure. Neurobiol Learn Mem 94:435–445.

738 Supple WF, Leaton RN, Fanselow MS (1987) Effects of cerebellar vermal lesions on species-specific fear
739 responses, neophobia, and taste-aversion learning in rats. PhysiolBehav 39:579–586.

740 Takahashi LK, Nakashima BR, Hong H, Watanabe K (2005) The smell of danger: a behavioral and neural
741 analysis of predator odor-induced fear. NeurosciBiobehav Rev 29:1157–1167.

742 Takemura M, Gomi H, Colucci-Guyon E, Itohara S (2002) Protective role of phosphorylation in turnover
743 of glial fibrillary acidic protein in mice. J Neurosci 22:6972–6979.

744 Timmann D, Drepper J, Frings M, Maschke M, Richter S, Gerwig M, Kolb FP (2010) The human
745 cerebellum contributes to motor, emotional and cognitive associative learning. A review. Cortex
746 46:845–857.

747 Vardjan N, Kreft M, Zorec R (2014) Dynamics of β-adrenergic/cAMP signaling and morphological changes
748 in cultured astrocytes. Glia 62:566–579.

749 Vialou V et al. (2010) DeltaFosB in brain reward circuits mediates resilience to stress and antidepressant
750 responses. Nat Neurosci 13:745–752.

751 Wang DO, Martin KC, Zukin RS (2010) Spatially restricting gene expression by local translation at
752 synapses. Trends Neurosci. 33:173-82

753 Wang M, Wang Q, Whim MD (2016) Fasting induces a form of autonomic synaptic plasticity that
754 prevents hypoglycemia. Proc Natl Acad Sci U S A 113:E3029-38

755 Widagdo J, Chai YJ, Ridder MC, Chau YQ, Johnson RC, Sah P, Huganir RL, Anggono V (2015) Activity-
756 Dependent ubiquitination of GluA1 and GluA2 regulates AMPA receptor intracellular sorting and
757 degradation. Cell Rep 10:783–795

758 Wulff P, Goetz T, Leppä E, Linden A-M, Renzi M, Swinny JD, Vekovischeva OY, Sieghart W, Somogyi P,
759 Korpi ER, Farrant M, Wisden W (2007) From synapse to behavior: rapid modulation of defined
760 neuronal types with engineered GABAA receptors. Nat Neurosci 10:923–929.

761

762

JNeurosci Accepted Manuscript

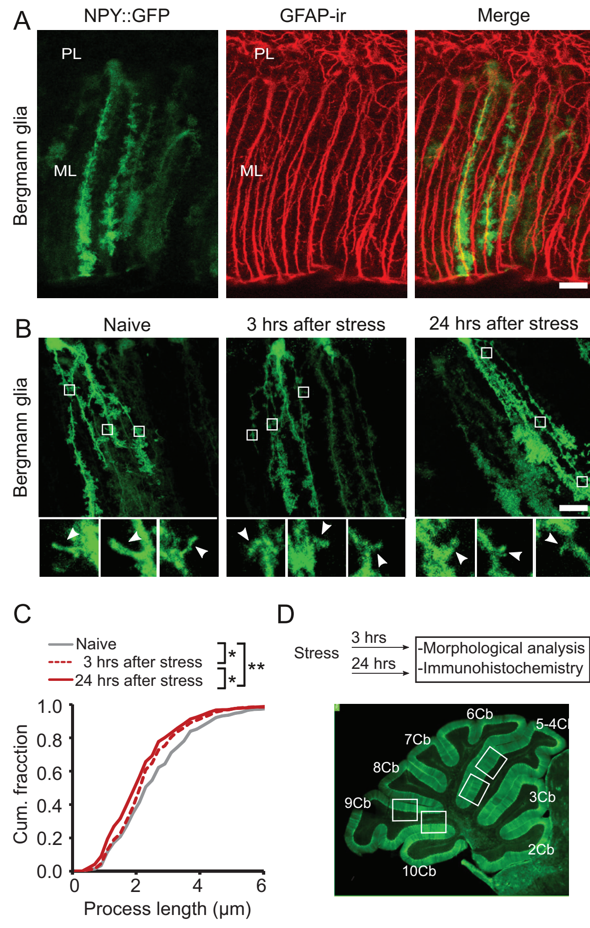

JNeurosci Accepted Manuscript

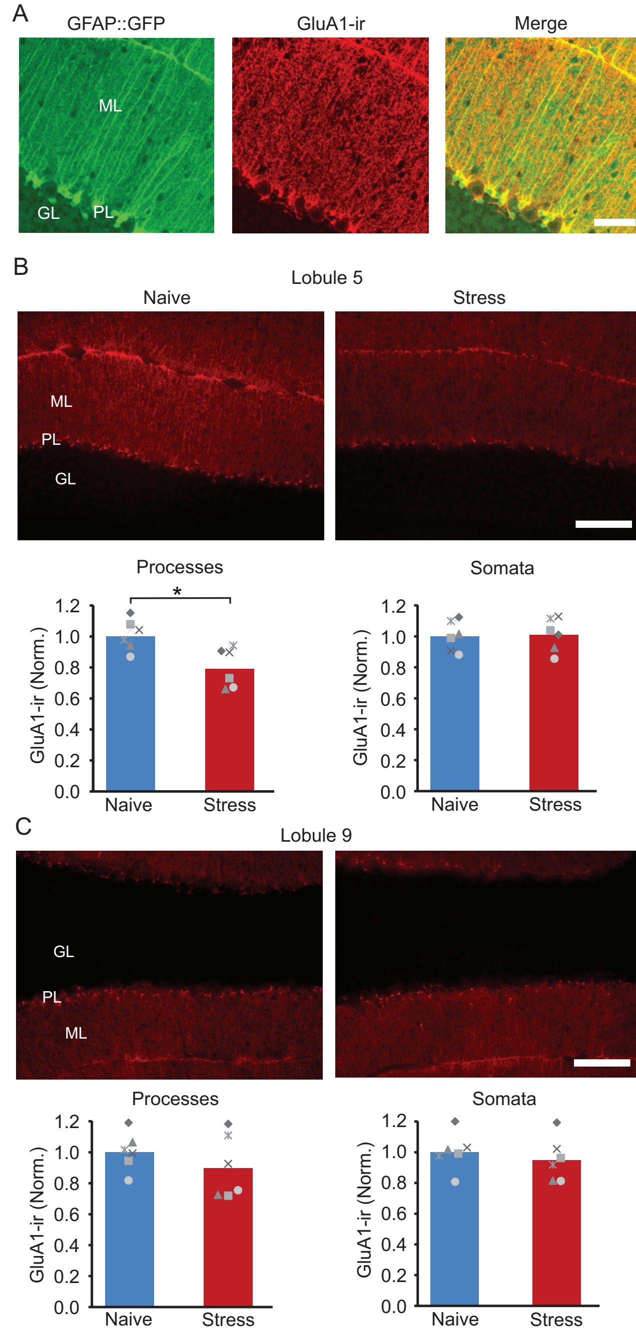

JNeurosci Accepted Manuscript

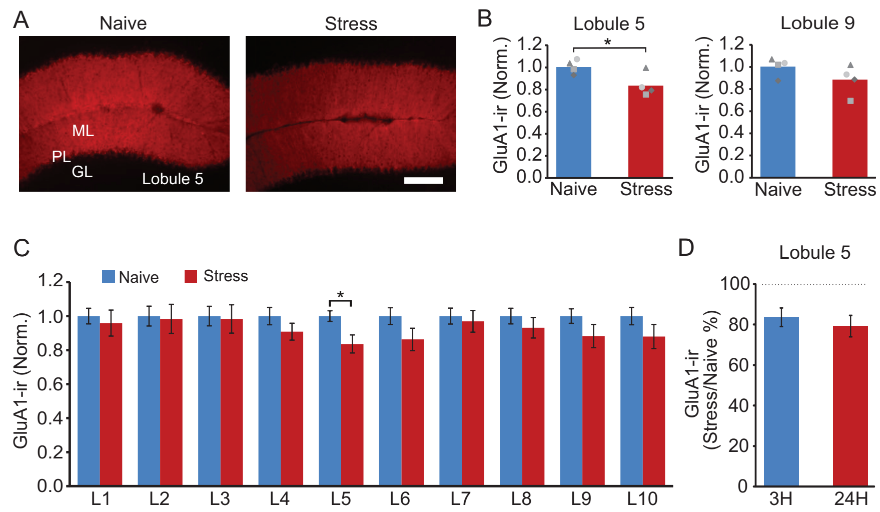

JNeurosci Accepted Manuscript

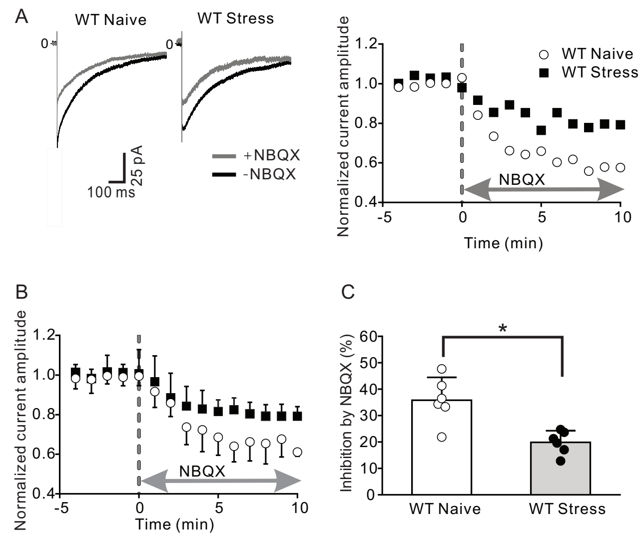

JNeurosci Accepted Manuscript

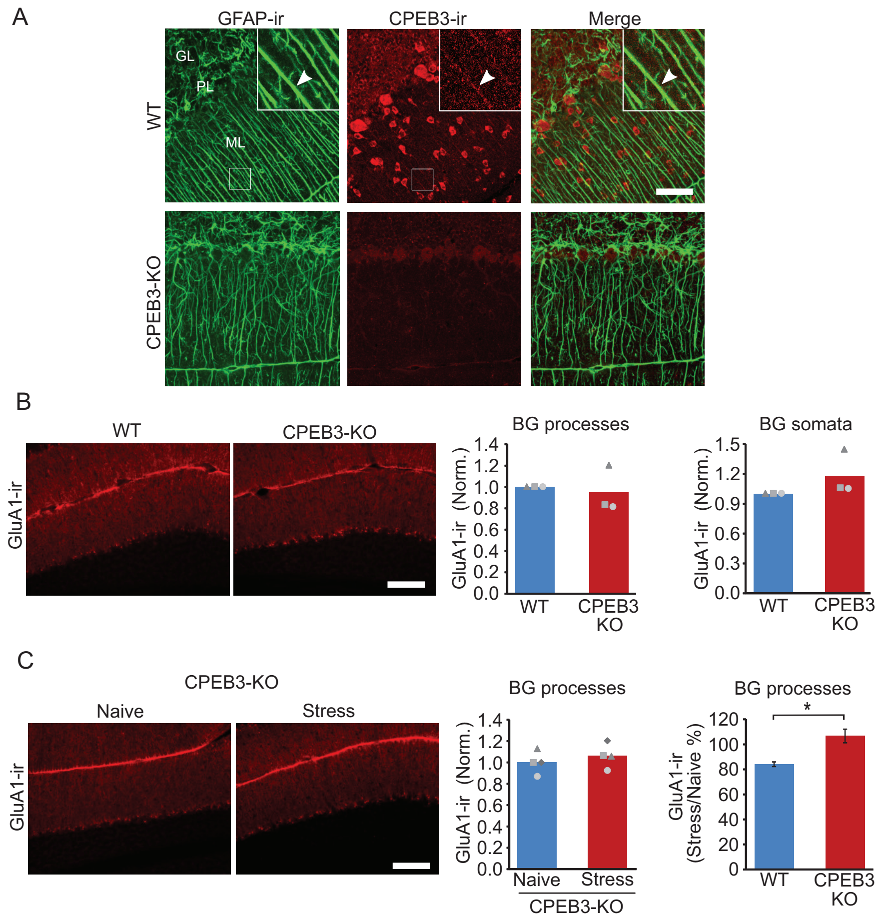

JNeurosci Accepted Manuscript

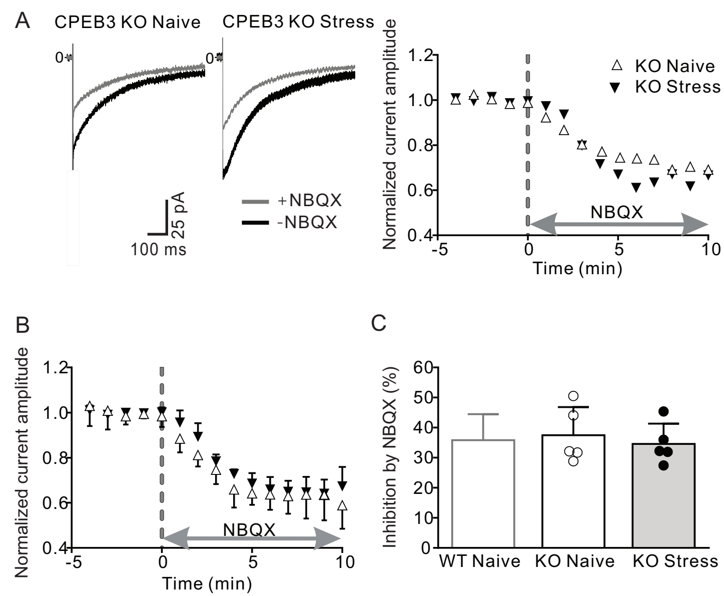

JNeurosci Accepted Manuscript

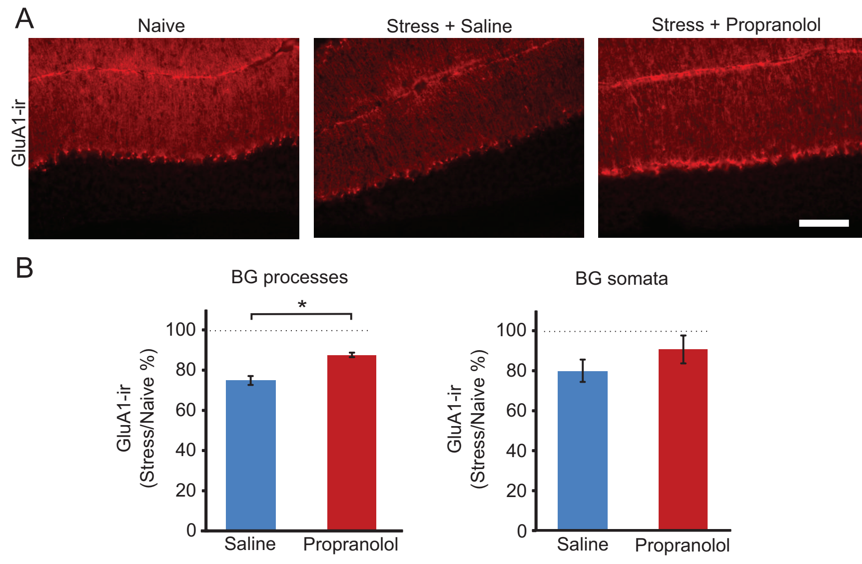

JNeurosci Accepted Manuscript